Principles and Practices of Si Light Emitting Diodes using Dressed Photons

M. Ohtsu[1] and T. Kawazoe[2]

[1]Research Origin for Dressed Photon,
c/o Nichia Corp., 3-13-19 Moriya-cho, Kanagawa-ku, Yokohama, Kanagawa 221-0022 Japan
[2]Tokyo Denki University,
5 Senju-Asahi-cho, Adachi-ku, Tokyo 120-8551, Japan

Abstract

This paper reviews basic research and technical developments on silicon (Si) light-emitting diodes (Si-LEDs) fabricated by using a novel dressed-photon–phonon (DPP) annealing method. These devices exhibit unique light emission spectral profiles in the wavelength range 900–2500 nm, including novel photon breeding features. The highest optical output power demonstrated was as high as 2.0 W. It is pointed out that boron (B) atoms, serving as p-type dopants, formed pairs whose length was three-times the lattice constant of the host Si crystal. These B atom pairs are the origin of the photon breeding. A phenomenological two-level two-state (TLTS) model is presented, revealing that the external electric and optical fields, applied during the DPP-assisted annealing, drastically decrease the height of the potential barrier between the two states. This decrease is the reason why the spatial distribution of B atoms is efficiently modified by the DPP-assisted annealing even at low temperature. The TLTS model and a stochastic model confirm that the optimum DPP-assisted annealing is realized by setting the ratio of the electron injection rate and the photon irradiation rate to 1:1. A phase diagram is presented as an aid for developing a novel theory for realizing more efficient and higher-power Si-LEDs.

1 Introduction

Crystalline silicon (Si) has long been a key material supporting the development of electronics engineering for more than half a century. However, because Si is an indirect-transition type semiconductor, it has been considered to be unsuitable for light-emitting devices. Because the bottom of the conduction band and the top of the valence band in Si are at different positions in reciprocal lattice space, the momentum conservation law requires an interaction between an electron–hole pair and phonons for radiative recombination; however, the probability of this interaction is low.

Nevertheless, Si has been the subject of extensive research on the fabrication of Si light-emitting devices. These include, for example, research using porous Si [1], a

super-lattice structure of Si and SiO_2 [2], and Si nanoprecipitates in SiO_2 [3]. However, the devices fabricated in these research studies have some limitations, such as low efficiency, the need to operate at low temperature, complicated fabrication processes, and the difficulty of current injection.

To solve these problems, a novel method that exploits the dressed photon (DP) has been invented [4,5]. The DP is a quantum field created when a photon couples with an electron–hole pair in a nanometric space. Theoretical studies have shown that a DP could excite multi-mode coherent phonons and couple with them to create a novel state called a dressed-photon–phonon (DPP) [4,6]. To realize a light-emitting diode (LED) by using crystalline Si, DPPs are used two times: first for device fabrication, and second for device operation.

In the present paper, first, the fabrication and operation of a Si-LED are described in Sections 2 and 3, respectively. Second, Sections 4 and 5 review a technique for controlling the spatial distribution of boron (B) atoms by using a novel DPP-assisted annealing method. Finally, the optimum condition for this annealing is presented in Section 6. A summary is given in Section 7. Note that this paper discusses the principle and method of realizing infrared Si-LEDs. Refer to ref. [7] for details of visible light Si-LEDs, Si-lasers, and LEDs fabricated using other indirect-transition-type semiconductors (SiC and GaP), and related devices, which have been developed by using DPP-assisted annealing.

2 Fabrication

For device fabrication, first, the surface of an n-type Si crystal is doped with B atoms to transform it to a p-type material for forming a p–n homojunction structure. Second, the Si crystal is annealed via Joule heat generated by current injection. During the annealing, the Si crystal surface is irradiated with light to create DPPs at the B atoms. This novel annealing has been called DPP-assisted annealing [7].

In early work on fabrication, an n-type Si crystal with low arsenic (As) concentration was used [5]. Recently, however, As atoms have been replaced by antimony (Sb) atoms (density, 1×10^{15} /cm^3) because Sb atoms, which are heavier than As and Si atoms, are more advantageous for localizing the created phonons, which can couple with a DP for creating a DPP more efficiently. The thickness and the electrical

resistivity of the n-type Si crystal were 625 μm and 5.0 Ωcm, respectively.

Two-step ion implantation was carried out to dope the Si with B atoms:

(1) First step: B atoms were implanted with an energy of 700 keV at a dose of $2.7\times10^{14}/cm^2$. The peak concentration of B atoms was $1\times10^{19}/cm^3$ at a depth of 1400 nm from the Si crystal surface.

(2) Second step: B atoms were implanted with an energy of 10 keV at a dose of $5.3\times10^{14}/cm^2$. The peak concentration of B atoms was $1\times10^{20}/cm^3$ at a depth of 45 nm from the Si crystal surface. This second doping step was advantageous for decreasing the resistivity at the crystal surface.

Mesh-electrode type and flip-chip type devices were fabricated to achieve higher current injection and efficient heat dissipation. These devices are described in the following subsections.

2.1 Mesh-electrode type LED

Figure 1 shows a photographic profile of the fabricated mesh-electrode type device [8,9]. A homogeneous flat film composed of Cr/Al/Au layers (thicknesses: 30/200/300 nm) was coated on the n-type surface of the Si crystal described above to serve as a cathode. A mesh film of Cr/Au (thicknesses: 30/300 nm) was coated on the p-type surface to serve as an anode. The crystal was diced to form devices with areal sizes of 1 mm × 1 mm, and these devices were bonded on a PCB substrate made of high-thermal-conductivity AlN. The diameters of the electric wires bonded to the devices were increased from the previously employed 25 μm [10] to 45 μm to avoid damage to the wires and electrodes during high current injection.

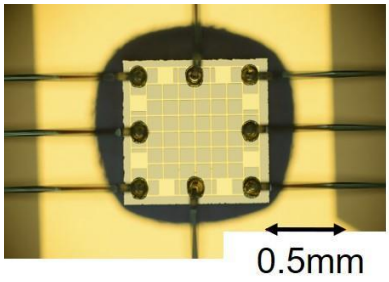

Fig. 1 Photographic profile of the fabricated mesh-electrode type LED.

The conditions for the DPP-assisted annealing were: (1) A substrate temperature of 285 K; (2) irradiation light with a wavelength of 1342 nm (photon energy $h\nu_{anneal}$ =

0.925 eV) and a power of 2.0 W; (3) injected current having a triangular waveform (50 s period) and a peak current of 1.3 A (current density 1.3 A/mm^2); and (4) an annealing time of 2 hours.

Since $h\nu_{anneal}$ is lower than the bandgap energy E_g of the Si crystal, the irradiated light is not absorbed by the Si crystal. Therefore, in the regions where DPPs are hardly created, B atoms diffuse simply due to the Joule heat generated by the applied electrical energy. However, in the regions where DPPs are easily created, the thermal diffusion rate of the B atoms becomes smaller via the following processes:

(1) Since the energy of the electrons driven by the forward-bias voltage is higher than E_g, the energy difference $E_{Fc} - E_{Fv}$ between the quasi Fermi energies in the conduction band E_{Fc} and the valence band E_{Fv} is larger than E_g. Therefore, the Benard–Duraffourg inversion condition is satisfied. Furthermore, since $h\nu_{anneal} < E_g$, the irradiated light propagates through the Si crystal without absorption and reaches the p–n homojunction. As a result, it creates DPPs efficiently at the B atoms. Since stimulated emission takes place via DPPs, the electrons create photons and are de-excited from the conduction band to the valence band via the phonon energy level.

(2) The annealing rate decreases because a part of the electrical energy for generating the Joule heat is spent for the stimulated emission of photons. As a result, at the regions where the DPPs are easily created, the B atoms become more difficult to diffuse.

(3) Spontaneous emission occurs efficiently at the regions in which the DPPs are easily created because the probability of spontaneous emission is proportional to that of stimulated emission. Furthermore, with the temporal evolution of process (2), the light from stimulated and spontaneous emission spreads through the whole Si crystal, and as a result, process (2) takes place autonomously throughout the entire volume of the Si crystal.

It is expected that this DPP-assisted annealing will form the optimum spatial distribution of the B atoms for efficient creation of DPPs, resulting in efficient LED operation. In a previous experimental study, temporal evolution of the temperature of the Si crystal surface was measured as annealing progressed [5]. After the temperature rapidly rose to 427 K, it fell and asymptotically approached a constant value (413 K) after 6 min, at which time the temperature inside the Si crystal was estimated to be about 573 K. The features of this temporal evolution are consistent with those of the principle

of the DPP-assisted annealing under light irradiation described above: The temperature rises due to the Joule heat generated by the applied electrical energy. However, the temperature gradually falls because stimulated emission is induced by the DPPs created at the B atoms. Finally, the system reaches the stationary state. This temporal decrease in the device temperature, and the temporal increase in the emitted light intensity, have been theoretically reproduced by a stochastic model of the spatial distribution of B atoms, which was controlled by DPPs [11].

2.2 Flip-chip type LED

To achieve higher injected current density than that of the mesh-electrode type device, a flip-chip type LED was fabricated [8,9]. First, its areal size was decreased. Second, larger-diameter electric wire was used. Third, a flip-chip structure was employed, in which the p-type layer was contacted to a PCB substrate for efficient heat dissipation.

Figure 2 shows a photographic profile of the fabricated device: A homogeneous flat film formed of Cr/Au/Ti/Pt/Au layers (thicknesses: 3/300/100/300/500 nm) was coated on the p-type surface of the Si crystal to serve as an anode. A patterned film of Cr/Au (thicknesses: 10/500 nm) was coated on the n-type surface as a cathode. The crystal was diced to form devices with areal sizes of 0.35 mm $\times$ 0.35 mm, which was smaller than that of the mesh-electrode type described in Subsection 2.1. This is equivalent to the size of commercially available devices made by using a conventional direct-transition type semiconductor. The diced device was bonded on a PCB substrate made of AlN. A single electric wire with a diameter as large as 60 μm was used to realize high-density current injection without any electrical damage.

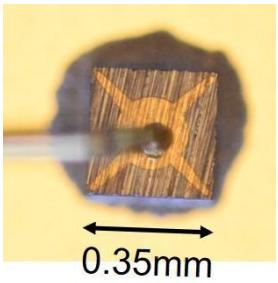

Fig. 2 Photographic profile of the fabricated flip-chip type LED.

The conditions for the DPP-assisted annealing were: (1) A substrate temperature of 289 K; (2) irradiation light with a wavelength of 1342 nm (photon energy $h\nu_{anneal}$ =

0.925 eV) and a power of 0.24 W (areal power density: 1.9 W/mm^2); (3) injected current with a triangular waveform (10 s period) and a peak current of 0.16 A (current density: 1.3 A/mm^2); and (4) an annealing time of 7.2 hours.

3 Operation

The operating principle of the fabricated Si-LED involves electron–hole pairs receiving enough momentum from coupled coherent phonons if the spatial distribution of B atoms in the p–n homojunction can be optimized for creating DPPs. Therefore, the light emission efficiency would be drastically increased by obeying the momentum conservation law.

For this operation, the light irradiation is no longer required; it is used only during the DPP-assisted annealing. Only forward current is injected, as in the case of conventional LED operation. This forward current causes an electron to be injected into the conduction band at the p–n homojunction, creating a photon by spontaneous emission even though its probability is very low. However, once this photon is created, it subsequently creates a DPP at the B atom in the p–n homojunction, and this DPP interacts with another electron in the conduction band to exchange momentum so that a secondary photon is created. By repeating these momentum exchange and photon creation processes, the emitted light intensity is amplified and reaches a stationary value within a short duration, so that sufficiently high-power light is emitted from the p–n homojunction.

It should be noted that photon breeding occurs during device operation [12]: The photon energy of the emitted light is equal to the photon energy $h\nu_{anneal}$ of the light irradiated during the annealing. (This is in contrast to a conventional device, where the photon energy of the emitted light is determined by E_g.) This is because the difference between $h\nu_{anneal}$ and E_g is compensated for by the energy of the created phonons. This compensation is possible because the spatial distribution of the B atoms has been controlled by the light irradiated during the DPP-assisted annealing, enabling the most efficient emission of photons with identical photon energy. In other words, the light irradiated during the DPP-assisted annealing serves as a “breeder” that creates photons with an energy equivalent to $h\nu_{anneal}$. This is the reason why this novel phenomenon is named photon breeding with respect to photon energy.

Photon breeding has been observed not only for the photon energy but also for

photon spin [13]. For example, linearly polarized light is emitted from the LED if it was fabricated by irradiating the LED with linearly polarized light during the annealing step. (Remember that the light emitted from a conventional LED is not polarized.)

The relationship between the forward-bias voltage (V) applied to the Si-LED and the injection current (I) indicated negative resistance [14]. This was due to the spatially inhomogeneous current density and the generation of filament currents. In other words, the B distribution had a domain boundary, and the current was concentrated in this boundary region. A center of localization where the electrical charge is easily bound was formed in this current concentration region, and a DPP was easily created there. That is, the negative resistance is consistent with the principle of the device fabrication described in Section 2.

3.1 Mesh-electrode type LED

Figure 3 shows the relations between the injected current (I) and the optical output power (P) of the upward-emitted light from the upper surface of the Si-LED, acquired at several substrate temperatures [8,9]. The figure shows that P is proportional to I^2 in the lower current region, whereas it is proportional to I^4 in the higher current region. The origin of this I^2-dependence has been attributed to the momentum transfer between localized phonons and electrons caused by electron–electron scattering [10]: In the case of a conventional LED fabricated with a direct-transition-type semiconductor, electron–electron scattering decreases the light emission efficiency. However, in the present Si-LED, this scattering process plays a different role. As will be explained in Section 4, the B atom pairs in the p–n homojunction are apt to stretch in a plane perpendicular to the [001] orientation of the Si crystal, i.e., perpendicular to the propagation direction of the light irradiated during the DPP-assisted annealing. Here, not only phonons but also electrons can be captured by these B atom pairs because they serve as cavity resonators for creating localized phonons. In other words, electrons can appear due to DPP-assisted annealing even in the area of the energy band structure where electrons cannot exist originally. Thus, two electrons could couple with localized phonons, leading to light emission by electron–electron scattering and the observed I^2-dependence of the emitted light power P.

The I^4-dependence originated in amplification by stimulated emission. By

defining the current at the boundary between the region of the I^2 - and I^4 -dependences as the threshold I_{th} , it is found that its value was lower at lower substrate temperatures. For example, it was 580 mA at 77 K. This means that the threshold current density was 0.58 A/mm^2, which is close to the threshold current density (0.20–0.35 A/mm^2) of a Si-laser fabricated by the DPP-assisted annealing [15]. The highest optical output power in Fig. 3 was 2.0 W with an injection current of 2.0 A and a substrate temperature of 77 K. This value is as high as 10^3-times that of a commercially available LED*.

*For example, the optical output power of a Hamamatsu Photonics device L12509-0155K, which is made of a direct-transition type semiconductor (InGaAs), is 2 mW. The peak emission wavelength is 1.55 μm.

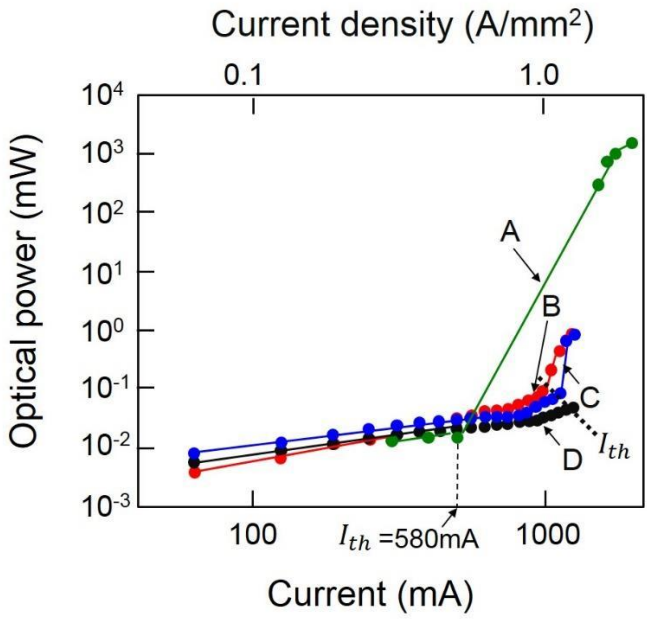

Fig. 3 Relations between the injection current and the optical output power.
Substrate temperatures were 77 K (A), 273 K (B), 290 K (C), and 293 K (D).

Figure 4 shows the spectral profile of the emitted light, which was acquired by cooling the substrate to 77 K and injecting a current of 2.0 A. In this figure, E_g represents the bandgap energy of the Si crystal at 77 K. This figure shows that the spectral profile has several peaks at $E_g - nE_{phonon}$, where n is an integer and E_{phonon}

is the phonon energy. The spectral peak at $E_g - 3E_{phonon}$ corresponds to the photon energy $h\nu_{anneal}$ of the light irradiated during the DPP-assisted annealing [13]. This correspondence is the photon breeding described in Subsection 2.1 [12]. Three phonons contribute to the light emission at $E_g - 3E_{phonon}$, because the length of the B atom pair is three-times the crystal lattice constant of Si. This figure also shows the higher harmonics of the phonon contributions, i.e., $E_g - 6E_{phonon}$ and $E_g - 9E_{phonon}$.

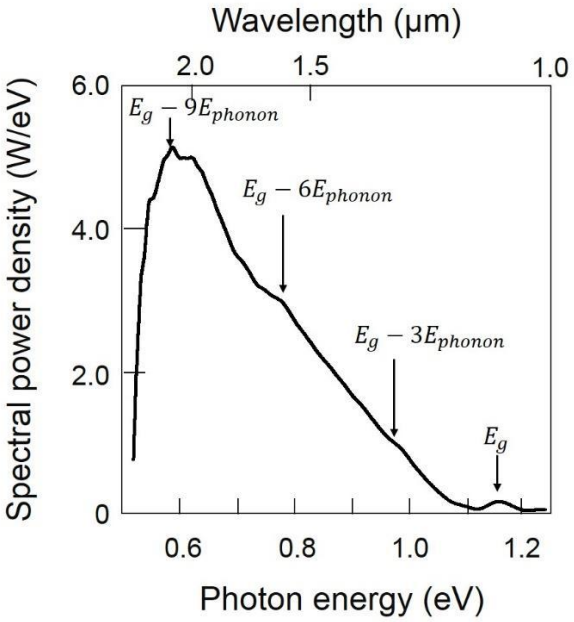

Fig. 4 Spectral profile of the emitted light at substrate temperature of 77 K.

3.2 Flip-chip type LED

Figure 5 shows the relations between I and P of the upward-emitted light from the upper surface of the Si-LED, acquired at several substrate temperatures. The highest optical output power in this figure was as high as 2.0 W at an injection current of 3.0 A and a substrate temperature of 77 K. This demonstrates that an extremely high optical output power density was achieved, as high as eight-times that of the mesh-electrode type LED described in Subsection 3.1.

The relations between I and P exhibited more complicated profiles than those in Fig. 3: In the low-current region [a], P increased slowly with increasing I,

whereas it increased rapidly in the high-current region [c]. The unique feature is that P decreased with increasing I in the intermediate region [b]. Figures 6(a)-(c) show photographs of the upward-emitted light spots in the regions [a]-[c], respectively. Among them, Fig. 6(b) shows that the light was emitted not only in the upward direction but also toward the side of the device. This side emission was attributed to the decrease in the observed value of P in region [b]. It should be noted that this side emission was due to stimulated emission, which suggests the possibility of super-luminescence or lasing operation.

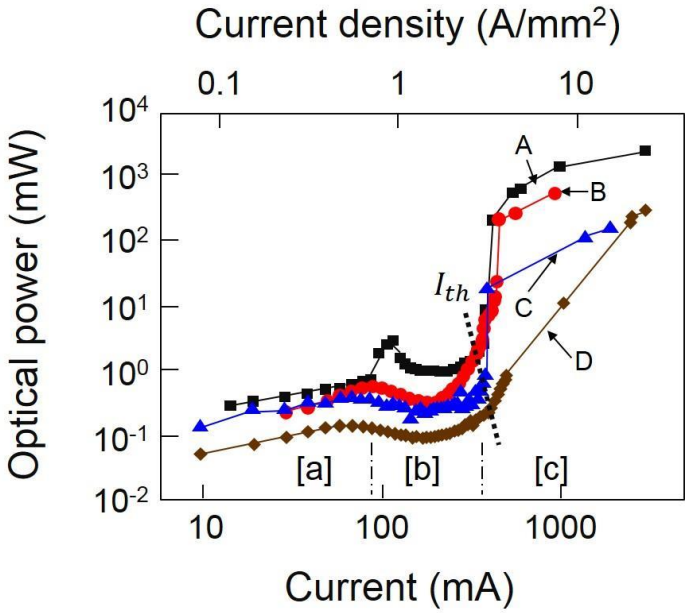

Fig.5 Relations between the injection current and the optical output power of the upward-emitted light from the surface of the Si-LED.

Substrate temperatures were 77 K (A), 195 K (B), 255 K (C), and 283 K (D).

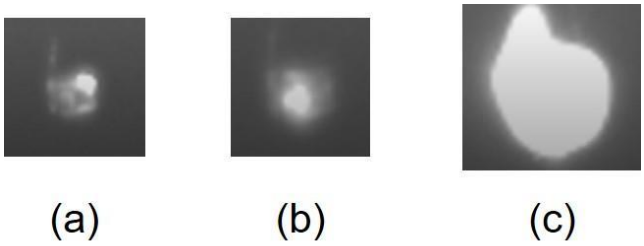

Fig.6 Photographs of the upward-emitted light spots.

(a), (b), (c) are images obtained in regions [a], [b], and [c] in Fig. 5, respectively.

As was the case in Fig. 3, the threshold I_{th} can be defined as the current at

the boundary between regions [b] and [c]. Figure 7 shows its dependence on the substrate temperature T. The solid line, fitted to the experimental results indicated by the closed circles, was expressed as $I_{th} = I_0 \exp(T / T_0)$. The characteristic temperature T_0 in this expression was 63 K, which corresponded to the energy of three phonons, $3E_{phonon}$, in the DPP. This means that the electron–hole pair was confined in the potential well formed by three phonons. This value of T_0 was as high as that of a conventional laser fabricated by a direct-transition type semiconductor (InGaAsP), lasing at a wavelength of 1.3 μm [16], which suggests that future progress in this work will realize highly reliable light-emitting devices using crystalline Si.

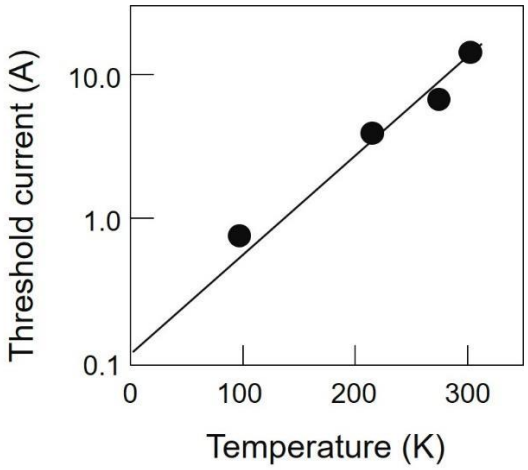

Fig. 7 Relation between the substrate temperature and the threshold current.

Figure 8(a) shows the spectral profile of the light emitted from the flip-chip type LED, which was acquired by cooling the substrate to 77 K and injecting a current of 3.21 A. Figure 8(b) shows the profile at a substrate temperature of 283 K and an injection current of 2.45 A. These figures also clearly demonstrate spectral peaks at $E_g - 3E_{phonon}$, $E_g - 6E_{phonon}$, and $E_g - 9E_{phonon}$, as was the case in Fig. 4.

4 Spatial distribution of boron

This section reviews the three-dimensional spatial distribution profile of the doped B

atoms formed as a result of the DPP-assisted annealing [13]. Atom probe field ion microscopy was used to acquire this distribution with sub-nanometer resolution [17]. It should be noted that the Si crystal is composed of multiple cubic lattices with a lattice constant a of 0.54 nm [18], and its top surface lies in the *xy*-plane (Fig. 9). The light irradiated during the DPP-assisted annealing is normally incident on this plane; i.e., the light propagation direction is parallel to the z-axis.

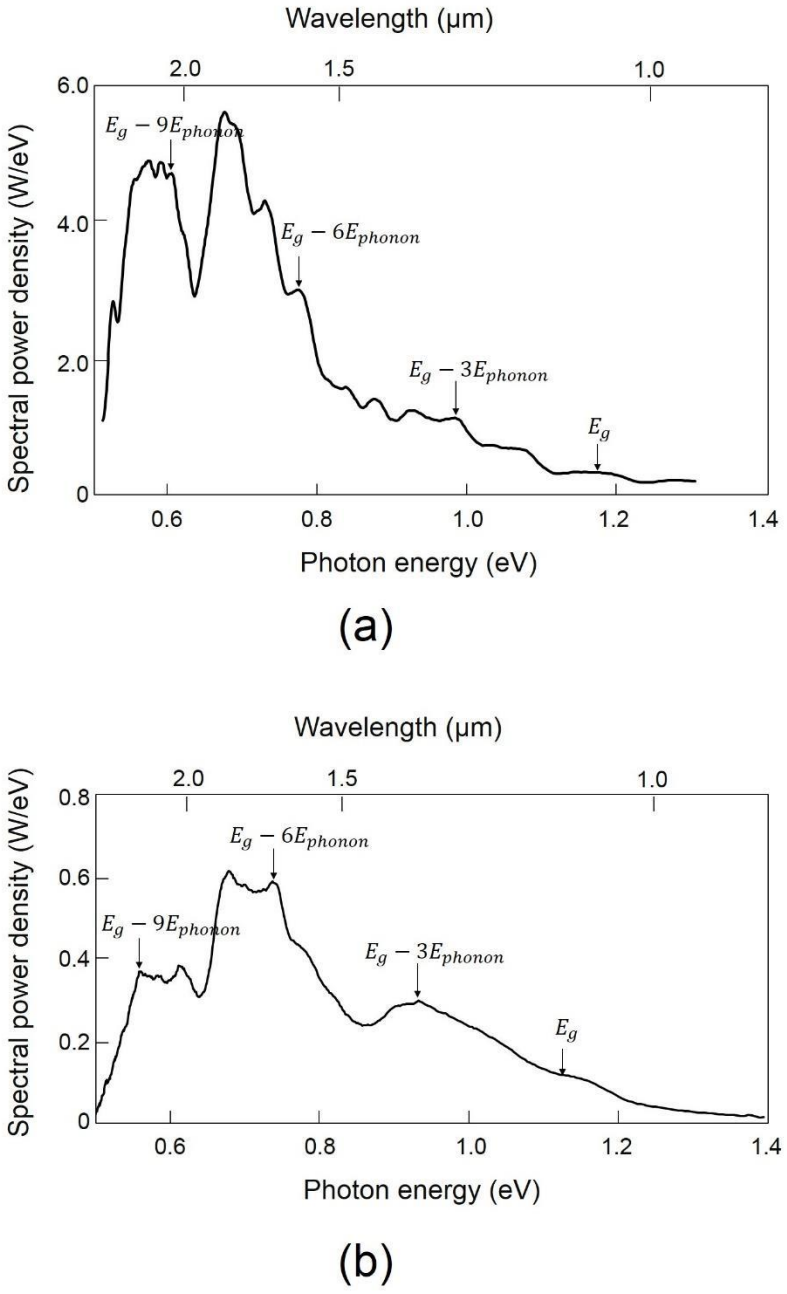

Fig. 8 Spectral profiles of the light emitted from the flip-chip type LED at substrate temperatures of 77 K (a) and 283 K (b).

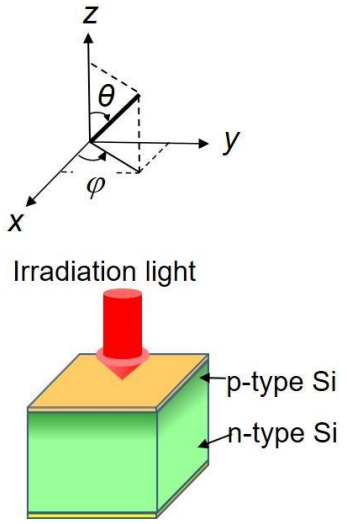

Fig. 9 Profile of the Si-LED under irradiation for the DPP-assisted annealing.

Some of the regularly arranged Si atoms are replaced by the doped B atoms in the DPP-assisted annealing. It has been pointed out that phonons can be localized at the B atoms for creating DPPs under light irradiation because the B atoms are lighter than the Si atoms. However, for this localization, it has also been pointed out that two or more adjacent B atoms (in other words, two or more unit cells containing B atoms) are required [19]. Since the doped B atom concentration is sufficiently low, making it difficult for more than three B atoms to aggregate, the following discussion considers two closely located adjacent B atoms (a B atom pair), at which a phonon is localized for creating a DPP. That is, the pair of unit cells containing the B atoms serves as a phonon localization center.

Figures 10(a) and (b) show the numbers of B atom pairs plotted as a function of the separation, d, between the B atoms in the pair, which were derived from the measurement results. Since the distribution of the number of B atom pairs is nearly random, it can be least-squares fitted by the Weibull distribution function (the solid curve in these figures). In the un-annealed Si crystal (Fig. 10(a)), the measured number of B atom pairs deviates from the solid curve in the range $d > 4.5$ nm. The deviation depends on the characteristics of the ion implantation.

In contrast, in the Si crystal after the DPP-assisted annealing (Fig. 10(b)), the deviation is much less than that in Fig. 10(a), which means that the DPP-assisted annealing modified the spatial distribution and decreased the deviation induced by the ion implantation, making the distribution more random. However, at specific values of

d ($=na$, where $n=3$, 4, 5, 6; refer to the four downward arrows in this figure), the number of B atom pairs still deviates from the solid curve and is larger than that of the solid curve. This is explained as follows: The B atom pair with the shortest d (i.e., equal to the lattice constant a) can orient in a direction parallel to the [100], [010], or [001] orientation because the Si crystal is composed of multiple cubic lattices. As a result, the momentum of the localized phonon points in this direction, which corresponds to the $\Gamma - X$ direction in reciprocal space. Thus, a photon is efficiently created because this $\Gamma - X$ direction is the same as the direction of the momentum of the phonon required for recombination between an electron at the bottom of the conduction band at the X-point and a hole at the top of the valence band at the Γ-point. Here, it should be noted that the absolute value of the momentum of the phonon has to be h/a for this electron–hole recombination to take place. Furthermore, it should also be noted that, among the phonons localized at the B atom pair with separation d ($=na$), the absolute value of the momentum of the lowest mode is h/na. By comparing these two absolute values, it is found that the DPP at this B atom pair has to create n phonons for recombination. Thus, it can be concluded that the four downward arrows in Fig. 10(b) indicate selective increases in the number of B atom pairs with separation $d=na$ due to the DPP-assisted annealing, and these pairs serve as localization centers for the phonons.

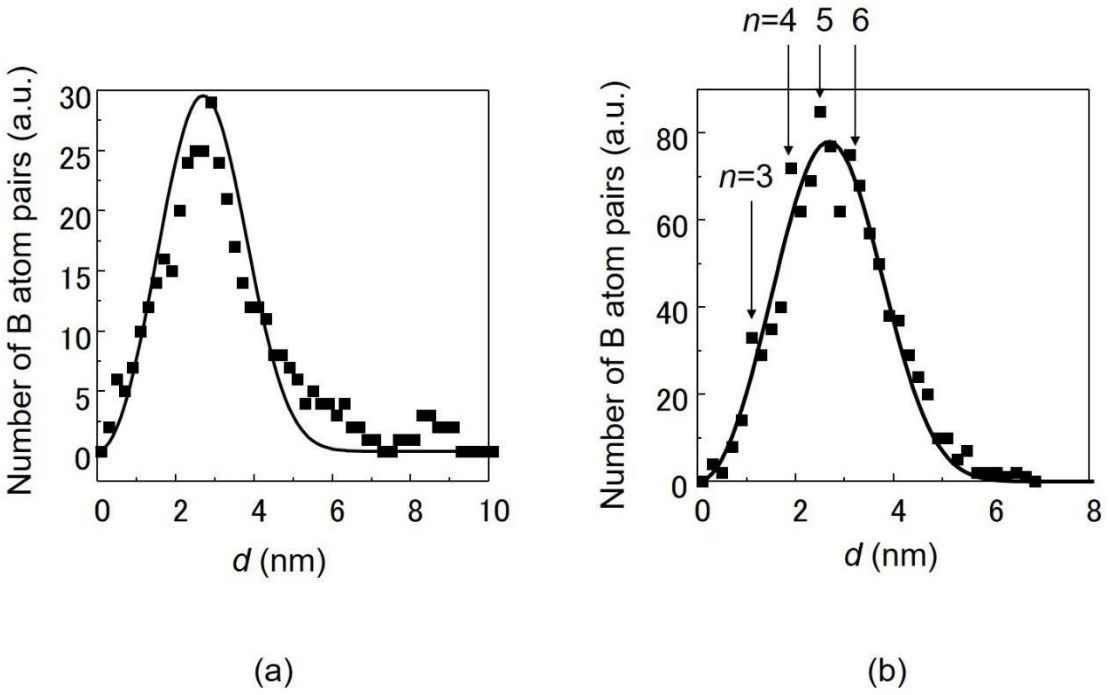

Fig. 10 Number of B atom pairs plotted as a function of the separation d between the B atoms in the pair. (a) The un-annealed Si crystal. (b) The Si crystal subjected to DPP-assisted annealing.

Figure 11(a) shows the spatial distribution of B atom pairs after the DPP-assisted annealing, which was recently acquired by improving the accuracy of atom probe ion microscopy [20]. The thick downward arrow in this figure clearly demonstrates that the deviation takes the maximum value at n=3, which means that B atom pairs most efficiently create three phonons for light emission, as is schematically shown in Fig. 11(b). As a result, the emitted photon energy $h\nu_{em}$ is expressed as $h\nu_{em} = E_g - 3E_{phonon}$. By substituting the values of E_g (= 1.12 eV) and the relevant optical mode phonon energy E_{phonon} (=65 meV [21]) into this equation, the value of $h\nu_{em}$ is derived to be 0.925 eV, which is identical to the photon energy $h\nu_{anneal}$ irradiated during the DPP-assisted annealing. This numerical relation is consistent with the experimental results in Figs. 4 and 8, which confirms that photon breeding with respect to photon energy occurs. The two thin downward arrows in Fig. 11(a) represent the values at $n = 6$ and $n = 9$, which correspond to $E_g - 6E_{phonon}$ and $E_g - 9E_{phonon}$, respectively, in Figs. 4 and 8.

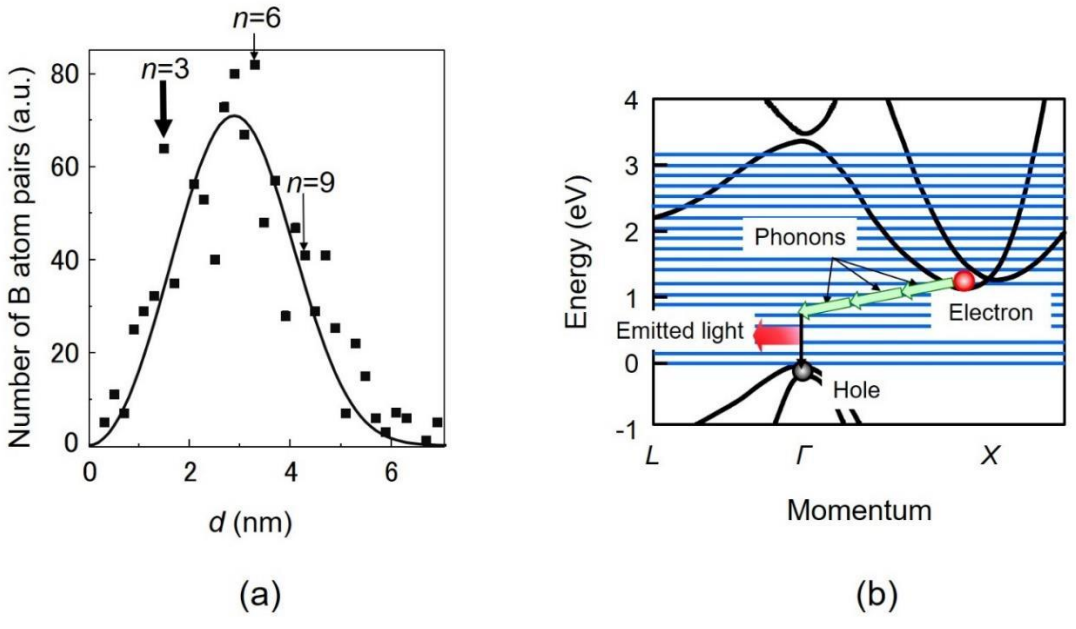

Fig. 11 (a) Number of B atom pairs, acquired by improving the measurement accuracy, and (b) the energy band structure of Si for schematically explaining light emission.

Figures 10(b) and 11(a) indicate selective increases in the number of B atom pairs with separation $d = na$. This means that, since n is an integer, B atom pairs are apt to orient along a plane perpendicular or parallel to the top surface of the Si crystal (zenith angle $\theta = 0°$ or $90°$). Orientation along other directions in which n is not an integer ($\theta \neq 0°, 90°$) hardly occurs. Figure 12 shows the relation between the zenith angle θ and the number of B atom pairs. It can be seen that this number takes the maximum value at $\theta = 90°$, which means that the B atom pairs in the p–n homojunction are apt to stretch in the *xy*-plane, which is perpendicular to the [001] orientation of the Si crystal, i.e., perpendicular to the propagation direction (*z*-axis) of the light irradiated during the DPP-assisted annealing. On the other hand, the number of B atom pairs takes the minimum value at $\theta = 0°$, which means that the B atom pairs hardly orient along the propagation direction (*z*-axis) of the light irradiated during the DPP-assisted annealing. This is because the phonons are hardly localized along this direction since their momenta are parallel to $\theta = 90°$ [22].

It is expected that photon breeding takes place not only with respect to photon energy, as described in Section 3, but also with respect to photon spin. That is, the light emitted from the LED can be polarized if the LED is fabricated by irradiating the Si crystal with polarized light during the DPP-assisted annealing. The fabrication method is the same as that described in Section 2, except that the irradiated light is linearly polarized along the x-axis. The diffusion of the B atoms was controlled by the linearly polarized light irradiated during the DPP-assisted annealing, with the result that the B atom pairs oriented along the y-axis . It has been experimentally confirmed that the degree of linear polarization increased with increasing DPP-assisted annealing time [13].

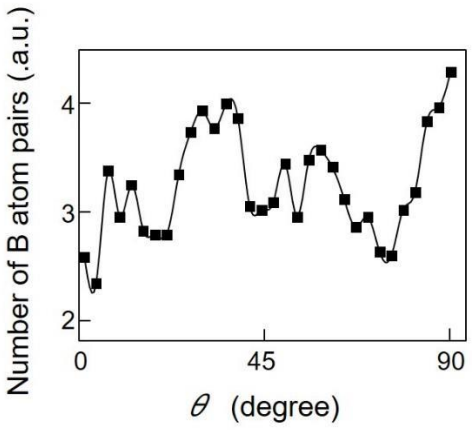

Fig. 12 Relation between the zenith angle θ and the number of B atom pairs.

Recent experimental work has confirmed that B atom pairs tend to form a chain-

like configuration [20]: Figures 13(a) and (b) show these configurations before and after the DPP-assisted annealing, respectively, which were acquired by the atom probe field ion microscopy. The short black arrows in these figures represent B atom pairs. The probability of one B atom pair existing in close proximity to the other pair in Fig. 13(a) was 0.743. In contrast, the probability in Fig. 13(b) increased to 0.788. The increase indicates that the B atom pairs tend to form a chain-like configuration. The red curves in these figures represent such a configuration.

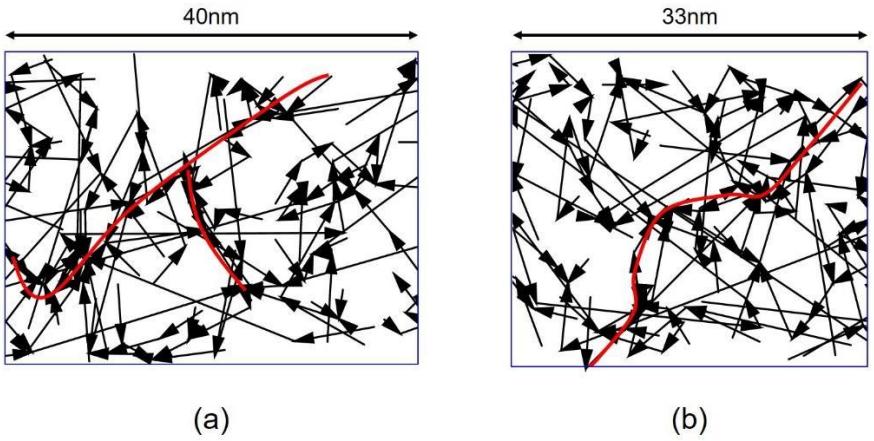

Fig. 13 Measured spatial distribution of B atom pairs, acquired before (a) and after (b) the DPP-assisted annealing.
The arrow in these figures represents the B atom pair. Red curves represent the chain-like configurations of the B atom pairs.

5 Effectiveness of the low-temperature DPP-assisted annealing

This section examines the reason why the spatial distribution of B atoms was effectively controlled by the DPP-assisted annealing at a temperature as low as 573 K, as presented in Subsection 2.1. For this examination, a two-level two-state (TLTS) model is used. This model has been adopted for accurately describing the spatial distribution of Zn atoms doped in a GaP-LED [23]. It enables evaluation of the potential barrier height of the electron, which is decreased by applying an external field. For reference, the details of the TLTS model have been reviewed in refs. [24,25].

Figure 14 shows the energy level diagram of the two-level system model [25]. The horizontal axis does not represent any specific physical quantity, whereas the vertical axis is the electron energy. The states A and B represent the electron states before

and after the DPP-assisted annealing, respectively. They are composed of two energy levels, i.e., the ground state ($\left|E_{gA}\right\rangle$,$\left|E_{gB}\right\rangle$) and the excited state ($\left|E_{exA}\right\rangle$,$\left|E_{exB}\right\rangle$), which respectively correspond to the valence and conduction bands in a semiconductor. The DPP-assisted annealing forces a forward transition from state A to state B. (The possibility of a backward transition from state B to state A is reviewed in Section 6.) The initial and final states of this forward transition are $\left|E_{gA}\right\rangle$ and $\left|E_{gB}\right\rangle$, respectively. Since the potential barrier V_g in the ground state is generally high, the transition takes place through the lower potential barrier V_{ex} in the excited state after excitation from $\left|E_{gA}\right\rangle$ to $\left|E_{exA}\right\rangle$. De-excitation from $\left|E_{exB}\right\rangle$ to the final state $\left|E_{gB}\right\rangle$ takes place after this transition.

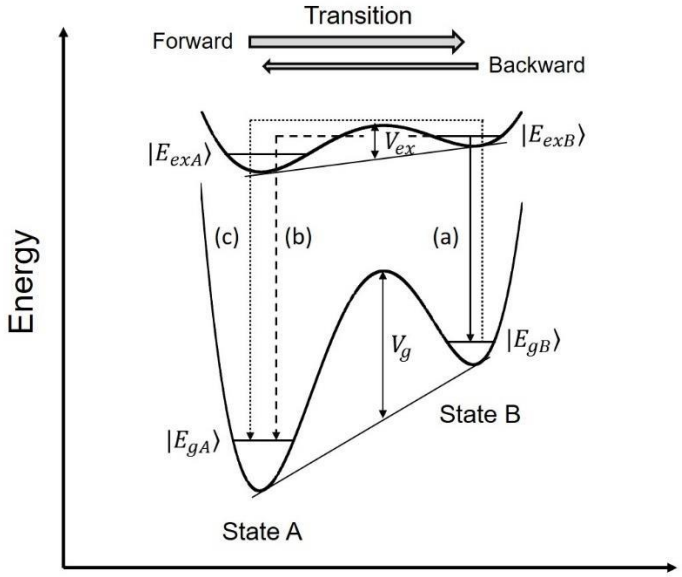

Fig. 14 The energy level diagram of the two-level two-state model.

The TLTS model can describe the DPP-assisted annealing rate, depending on which state the electron is in:

State A: State A corresponds to the region in the Si crystal where the spatial distribution of B atoms is not suitable for generating DPPs. Therefore, the electron in $\left|E_{exA}\right\rangle$

generates Joule heat. On the other hand, the electron in $|E_{gA}\rangle$ is excited by absorbing the irradiated light, and, as a result, Joule heat is also generated. Because of the Joule heat generated in these cases, the annealing rate is higher in state A.

State B: State B corresponds to the region in the Si crystal where the spatial distribution of B atoms is suitable for generating DPPs. Since electron–hole pairs can radiatively recombine in this case, the light irradiated during the DPP-assisted annealing triggers stimulated emission. As a result, the annealing rate is lower in state B because the stimulated emission optical energy dissipates from inside the Si crystal to the outside.

Due to the difference in the annealing rates in states A and B, the spatial distribution of B atoms changes autonomously. When it reaches that of state B, the DPP-assisted annealing is completed, and the Si-LED is thus fabricated. It has been experimentally confirmed for a GaP-LED that the external electric and optical fields applied during the DPP-assisted annealing drastically decreased the value of $V_{ex}{}^{*}$.

This decrease is the reason why the spatial distribution of B atoms was efficiently modified by the DPP-assisted annealing even at low temperature, as described in Subsection 2.1 (573 K). In other words, the outstanding technical advantage of the DPP-assisted annealing is that it does not require any high-temperature electric furnaces, which have been needed for conventional thermal annealing.

---

* In the absence of an external field, the value of V_{ex} that electrons in the doped Zn atoms must exceed to make a transition inside the GaP crystal was 0.61 eV. The value obtained when Ga sites were substituted via the kick-out mechanism was 1.64 eV [26]. However, with the external fields, it was estimated to be as low as 0.48 eV [23].

---

6. Optimum condition for DPP-assisted annealing

This section presents the optimum condition for DPP-assisted annealing, i.e., the optimum ratio between the electron injection rate and the photon irradiation rate for DPP-assisted annealing [23]. First, the electron is assumed to be in the excited or ground state of state B ($|E_{exB}\rangle$ or $|E_{gB}\rangle$) in Fig. 14 as a result of DPP-assisted annealing, i.e.,

as a result of the forward transition from state A to state B. Next, the solid, broken and dotted arrows (a)–(c) in Fig. 14 represent the possible paths of the electron for de-excitation, excitation, and backward transition via photon emission and absorption, which may subsequently occur by continuing the DPP-assisted annealing.

Path (a): The electron in $|E_{exB}\rangle$ can emit a photon via spontaneous or stimulated emission. Thus, it de-excites to $|E_{gB}\rangle$ without a transition back to state A.

Path (b): If the electron in $|E_{exB}\rangle$ does not emit a photon, it transitions back to $|E_{exA}\rangle$ in state A, and subsequently de-excites to $|E_{gA}\rangle$ via nonradiative relaxation.

Path (c): The electron in $|E_{gB}\rangle$ is excited to $|E_{exB}\rangle$ by absorbing a photon. It subsequently transitions back to $|E_{exA}\rangle$ in state A and de-excites to $|E_{gA}\rangle$ via nonradiative relaxation, as in path (b).

In the case of path (a), the spatial distribution of B atoms remains unchanged even though DPP-assisted annealing proceeds, because both the initial and final states ($|E_{exB}\rangle$ and $|E_{gB}\rangle$) are in state B. However, in the case of paths (b) and (c), the final state $|E_{gA}\rangle$ is in state A, and this spatial distribution easily changes as DPP-assisted annealing proceeds. Thus, to confine the electrons in state B, paths (b) and (c) must be blocked to prevent the backward transition.

Noting that a photon causes an electron to emit another photon via stimulated emission, a promising method for blocking the paths is to set the ratio of the electron injection rate and the photon irradiation rate to 1:1, which corresponds to the optimum condition for the DPP-assisted annealing. If the electron injection rate is higher than the photon irradiation rate, the excess electrons do not emit photons via stimulated emission but escape through path (b). On the other hand, if the photon irradiation rate is higher than the electron injection rate, the excess photons do not cause electrons to emit photons via stimulated emission but allow the electrons to escape through path (c).

Experiments have been carried out to confirm this optimum condition by using a GaP-LED as a specimen [23]. The experimental results showed that the rate of increase in the emitted light intensity due to the DPP-assisted annealing took the maximum value

when the ratio between the photon number and the electron number was 1.3:1, which is approximately 1:1. This clearly shows the optimum condition claimed above. This optimum condition has been theoretically reproduced by a stochastic model of the spatial distribution of B atoms, which was controlled by the DPPs [11].

This optimum condition suggests that conventional thermal annealing, i.e., by heating the sample in an electric furnace, is not compatible with fabricating novel devices having photon breeding features even if the furnace temperature can be increased to much higher than the value given in Subsection 2.2 (573 K). DPP-assisted annealing is the only suitable fabrication method.

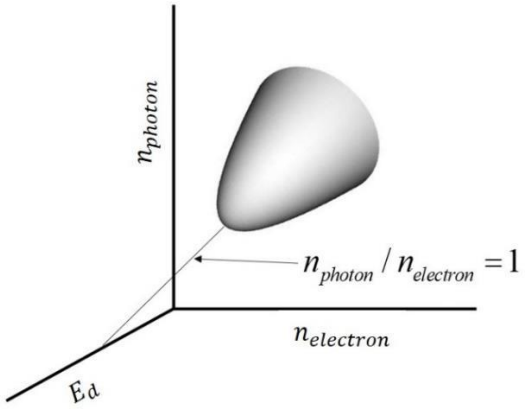

Fig. 15 Phase diagram for representing the area in which the rate of increase in the emitted light intensity due to the DPP-assisted annealing is high.

The gray cone in the phase diagram of Fig. 15 represents the area in which the rate of increase in the emitted light intensity due to the DPP-assisted annealing is high, which was empirically illustrated through experiments and the discussion on the optimum condition above. Here, $n_{electron}$ and n_{photon} are the electron injection rate and the photon irradiation rate, respectively. It should be pointed out that the rate of increase is the largest when $n_{photon} / n_{electron} = 1$, as was discussed above. In this figure, E_d is the magnitude of the dissipated optical energy. It is the magnitude of the energy of the stimulated emission, which is emitted from the electron that jumped into the DPP field.

Since this light propagates out from the Si crystal, the diffusion rate of the B atoms locally decreases around this DPP field, by which the spatial distribution of the B atom pairs is autonomously controlled to promote the DPP-assisted annealing.

A novel theory is required since one of the major requests from experimentalists is to find the optimum condition for realizing the highest efficiency of creation and measurement of DPs. It is expected that Fig. 15 will serve as a reference to find such an optimum condition.

7 Summary

After reviewing fabrication of Si-LEDs using a novel DPP-assisted annealing method, their unique light emission spectral profiles were presented in the wavelength range 900–2500 nm, including novel photon breeding features. The highest optical output power demonstrated was as high as 2.0 W, which was 10^3-times that of a conventional LED.

It was experimentally found that the B atoms formed pairs as a result of the DPP-assisted annealing, and the length of these pairs was three-times the lattice constant of the Si crystal. The pairs extended in a plane perpendicular to the propagation direction of the light irradiated during the DPP-assisted annealing. These B atom pairs were confirmed to be the origin of the photon breeding. It was also found that photon breeding took place with respect to photon spin. Recent measurements confirmed that the B atom pairs tend to form a chain-like configuration.

A phenomenological two-level two-state (TLTS) model confirmed that the external electric and optical fields applied during the DPP-assisted annealing drastically decreased the height of the potential barrier between the two states. This decrease was the reason why the spatial distribution of B atoms was efficiently modified by the DPP-assisted annealing even at low temperature. The TLTS model and a stochastic model confirmed that the optimum DPP-assisted annealing was realized by setting the ratio of the electron injection rate and the photon irradiation rate to 1:1, which was also confirmed experimentally.

A phase diagram was presented as an aid for developing a novel theory for finding the optimum condition for the highest efficiency of creation/measurement of DPs and for realizing more efficient and higher-power Si-LEDs.

References

[1] K.D. Hirschman, L.Tysbekov, S.P. Duttagupta, and P.M. Fauchet, “Silicon-based visible light-emitting devices integrated into microelectronic circuits,” Nature, **384** (1996) pp.338-341.

[2] Z.H. Lu, D.J. Lockwood, and J.-M. Baribeau, Nature, “Quantum confinement and light emission in SiO_2/Si Superlattices,” Nature, **378** (1995) pp.258-260.

[3] T. Komoda, J. Kelly, E. Cristiano, A. Nejim, P. L. F. Hemment, K. P. Homewood, R. Gwilliam, J. E. Mynard, and B. J. Sealy, “Visible photoluminescence at room temperature from micro- crystalline silicon precipitates in SiO_2 formed by ion implantation,” Nucl. Instrum. and Methods in Phys. Res. Sect.B, **96** (1995) pp.387-391.

[4] M. Ohtsu, “Dressed photon technology,” Nanophotonics **1**, (2012) pp.83-97.

[5] T. Kawazoe, M. Mueed, and M. Ohtsu, “Highly efficient and broadband Si homojunction structured near-infrared light emitting diodes based on the phonon-assisted optical near-field process,” Appl. Phys. B **104**, (2011) pp.747-754.

[6] Y. Tanaka and K. Kobayashi, “Optical near field dressed by localized and coherent phonons,” J. Microscopy **229** (2008) pp.228-232.

[7] M. Ohtsu, *Silicon Light-Emitting Diodes and Lasers* (Springer, (Springer, Heidelberg 2006), pp. 1-138.

[8] T. Kawazoe and M. Ohtsu, “Operation with 1W-optical output of Si-LED and current dependence,” Abstracts of the 65th Jpn. Soc. Appl. Phys. Spring Meeting, March 2018, Tokyo, Japan, paper number 19p-F310-13.

[9] M. Ohtsu and T. Kawazoe, “High-Power Infrared Silicon Light-emitting Diodes Fabricated and Operated using Dressed Photons,” Off-shell Archive, Offshell:1804O.001.v1.

[10] J.H. Kim, T. Kawazoe, and M.Ohtsu, "Dependences of emission intensity of Si light-emitting diodes on dressed-photon—phonon-assisted annealing conditions,”Appl. Phys. A , **123**,606 (2017).

[11] M. Katori and H. Kobayashi, “Nonequillibrium Statistical Mechanical Models for Photon Breeding

Processed Assisted by Dressed-Photon—Phonons," *Prog. In Nanophotonics* 4 (ed. By M. Ohtsu and T. Yatsui) (Springer, Heidelberg, 2017) pp.19-55.

[12] M. Ohtsu, *Silicon Light-Emitting Diodes and Lasers*, (Springer, Heidelberg, 2016), pp.8-10.

[13] T. Kawazoe, K. Nishioka, and M. Ohtsu, "Polarization control of an infrared silicon light-emitting diode by dressed photons and analyses of the spatial distribution of doped boron atoms," Appl. Phys.A , **121** (2015) pp. 1409-1415.

[14] E.Shl, *Nonequilibrium Phase Transitions in Semiconductors* (Springer, Heidelberg 1987), pp. 5-6.

[15] T. Kawazoe, K. Hashimoto, and S. Sugiura, "High-power current-injection type Silicon laser using nanophotonics," Abstract of the EMN Nanocrystals Meeting, October 17-21, 2016, Xi'an, China, pp.9-11 (paper number 03).

[16] R.Adams, M.Asada, Y.Suematsu, and S.Arai, "The Temperature Dependence of the Efficiency and Threshold Current of $In_{1-x}Ga_xAs_yP_{1-y}$ Lasers Related to Intervalence Band Absorption," Jpn. J. Appl. Phys., **19** (1980) pp.L621-L624.

[17] K. Hono, "Nanoscale microstructural analysis of metallic materials by atom probe field ion microscopy, " Prog. Mater. Sci. **47** (2002) pp.621–729.

[18] K. Godwod, R. Kowalczyk, and Z. Szmid, "Application of a precise double X-ray spectrometer for accurate lattice parameter determination," Phys. Stat. Sol. (a), **21** (1974) pp.227-234.

[19] M. Ohtsu, *Dressed Photons* (Springer, Heidelberg, 2014), pp. 62-67.

[20] T. Kawazoe, J.H. Kim, and M. Ohtsu, "Regularity of Boron dopant distribution in a Si-crystal annealed by the dressed photon-phonon assisted annealing," *Abstract of the 77th Japan. Soc. Appl. Phys. Autumn Meeting*, (Niigata, Japan, 2016), 16a-B12-4.

[21] E. Anastassakis, A. Pinczuk, E. Burstein, F.H. Pollak, and M. Cardona, "Effect of static uniaxial stress on the Raman spectrum of silicon," Solid State Commun. **8** (1970) pp.133-138.

[22] Y. Shinohara, T. Otobe, J. Iwata, K. Yanaba, "First-Principles Calculation to Explore Mechanisms of Coherent Phonon Generation," J. Phys. Soc. Jpn. **67** (2012) pp.685-689.

[23] J. H. Kim, T. Kawazoe, and M. Ohtsu, "Optimization of dressed-photon—phonon-assisted annealing for fabricating GaP light-emitting diodes," Appl. Phys. A **121** (2015) pp.1395-1401.

[24] R. Jankowiak, R. Richert, and H. Bässler, "Nonexponential hole burning kinetics in organic glasses," J. Phys. Chem. **89** (1985) pp 4569-4574.

[25] W. Köhler, J. Meiler, and J. Friedrich, "Tunneling dynamics of doped organic low-temperature glasses as probed by a photophysical hole-burning system," Phys. Rev. B **35** (1987) pp.4031-4037.

[26] A. Höglund, C. Castleton, and S. Mirbt, “Diffusion mechanism of Zn in InP and GaP from first principles,”Phys. Rev.B **77** (2008) 113201.